

RSC Advances



This is an *Accepted Manuscript*, which has been through the Royal Society of Chemistry peer review process and has been accepted for publication.

Accepted Manuscripts are published online shortly after acceptance, before technical editing, formatting and proof reading. Using this free service, authors can make their results available to the community, in citable form, before we publish the edited article. This *Accepted Manuscript* will be replaced by the edited, formatted and paginated article as soon as this is available.

You can find more information about *Accepted Manuscripts* in the [Information for Authors](#).

Please note that technical editing may introduce minor changes to the text and/or graphics, which may alter content. The journal's standard [Terms & Conditions](#) and the [Ethical guidelines](#) still apply. In no event shall the Royal Society of Chemistry be held responsible for any errors or omissions in this *Accepted Manuscript* or any consequences arising from the use of any information it contains.



Journal Name

ARTICLE

Electrodeposition synthesis of reduced graphene oxide-carbon nanotube hybrids on indium tin oxide electrode for simultaneous electrochemical detection of ascorbic acid, dopamine and uric acid†

Received 00th January 20xx,
Accepted 00th January 20xx

DOI: 10.1039/x0xx00000x

www.rsc.org/

Yong Zhang,^{ab} Ye Ji,^a Ziying Wang,^a Sen Liu^{*a} and Tong Zhang^{*ab}

Reduced graphene oxide-carbon nanotube (rGO-CNT) hybrids have been synthesized by electrodeposition of GO stabilized CNT using indium tin oxide (ITO) as working electrode, followed by electrochemical reduction of GO-CNT into rGO-CNT on the surface of ITO. The combined characterizations of scanning electron microscope (SEM) and X-ray photoelectron spectroscopy (XPS) analysis have been used to examine the structure of rGO-CNT hybrids, indicating the successful preparation of hybrids. More importantly, compared with the bare ITO and rGO/ITO electrodes, the rGO-CNT/ITO electrode exhibits excellent sensing performance for electrochemical detection of ascorbic acid (AA), dopamine (DA) and uric acid (UA), leading to a high-performance electrochemical sensor for simultaneous detection of AA, DA and UA. The linear detection ranges of the AA, DA and UA sensors based on rGO-CNT hybrids were estimated to be 10–200 μM , 0.2–8.0 μM and 0.2–16.0 μM , and the detection limits were 5.31 μM , 0.04 μM and 0.17 μM , respectively.

Introduction

Ascorbic acid (AA), dopamine (DA) and uric acid (UA) are most important vitamins, important neurotransmitter and important metabolic end-product of purine, respectively. More importantly, AA, DA and UA play a significant role in the function of human metabolism, and the abnormal concentration levels of AA, DA and UA will lead to diseases such as scurvy, Parkinson's disease and gout.^{1–3} Hence, the determination of concentration levels of AA, DA and UA has a special meaning to guarantee health conditions. Up to now, many techniques have been used to detect these biomolecules. Particularly, the electrochemical technique has been proven as a promising technique for AA, DA and UA detection due to its excellent advantages such as cost-effectiveness, fast response, good stability, high sensitivity and selectivity.^{4–6}

It is well known that AA, DA and UA usually coexist in biological samples. What is more, AA, DA and UA have similar oxidation potentials at conventional electrodes for electrochemical detection, resulting in difficult electrochemical

identification. Fortunately, recent researches have shown that some novel functional materials exhibit good performances for electrochemical detection for AA, DA or UA.^{7,8} However, most of these materials could only selectively detect one of biomolecules. Thus, fabrication of three individual electrochemical sensors is involved for detection of AA, DA and UA, where the shortcoming of complicated, expensive and time consuming process limits their wide applications. To overcome this problem, simultaneous electrochemical detection of AA, DA and UA has been developed.^{9,10} However, AA, DA and UA have similar electrochemical properties and the complicated electrochemical identification in biological environment need be faced. Hence, developing a rapid, simple, accurate and reliable approach to simultaneously detect AA, DA and UA is highly desired.

In general, a modified electrode with excellent electrochemical performances needs to be designed by consideration of working electrode and sensing materials. To date, a variety of working electrodes, such as glassy carbon electrode (GCE),^{11,12} carbon paste electrode,^{13,14} pyrolytic graphite electrode^{15,16} and Pt electrode,¹⁷ have been used for simultaneous electrochemical detection of AA, DA and UA. The GCE has been widely used as working electrode due to its advantages of good conductivity, good chemical stability, high intensity and rigidity, which ensure that it is very easy to modify by sensing materials operated in the laboratory.^{18–22} On the other hand, indium tin oxide (ITO) also has remarkable physical and chemical properties as working electrode. Additionally, ITO is a low-cost material and more suitable for mass production and practical application. However, reports on development of modified ITO electrode for simultaneous

^aState Key Laboratory of Integrated Optoelectronics, College of Electronic Science and Engineering, Jilin University, Changchun, P. R. China

^bState Key Laboratory of Transducer Technology, Chinese Academy of Sciences, P. R. China

*Corresponding authors: E-mail: liusen@jlu.edu.cn (S. Liu); zhangtong@jlu.edu.cn (T. Zhang); Fax: +86 431 85168270; Tel: +86 431 85168385

† Electronic Supplementary Information (ESI) available: Details of preparation of GO, CVs of ITO in GO-CNT dispersion, CVs of GO-CNT/ITO in PBS, CVs of CNT/ITO in potassium ferricyanide solution and in PBS containing AA, DA and UA, CVs of rGO-CNT/ITO at different scan rates, DPV of CNT/ITO in PBS containing AA, DA and UA, DPVs of rGO-CNT/ITO in PBS containing AA, DA, UA and several co-existing substances, comparison of results, detection of AA, DA and UA at rGO-CNT/ITO in urine sample. See DOI: 10.1039/x0xx00000x

electrochemical detection of AA, DA and UA have been few reported so far.²³

It is well known that development of novel sensing materials has been proven as an effective method to fabricate electrochemical sensors for simultaneous detection of AA, DA and UA. For example, the organic polymers such as poly(vinyl alcohol) or poly(sulfonazo III) modified GCE shows good performances for simultaneous electrochemical detection of AA, DA and UA.^{24,25} However, the shortcomings including using environmental unfriendly organic solvents during preparation processes, and poor electrochemical conductivity limit their further applications. Furthermore, noble metals (such as PtAu alloy²³ and Pd-Pt nanocomposites²⁶) and metal oxide (such as LaFeO₃ nanofibers²⁷ and MgO nanostructures²⁸) could also be used for simultaneous electrochemical detection of AA, DA and UA. However, the expensive price of noble metals and the unsatisfactory electronic conductivity of metal oxides also restrict their further applications.

Compared with the above materials, carbon-based materials are more promising materials for simultaneous electrochemical detection of AA, DA and UA. Up to now, carbon-based materials such as nitrogen doped porous carbon nanopolyhedra,² single-walled carbon nanohorn,³ hollow nitrogen-doped carbon microspheres⁴ and carbon nanotube (CNT)²⁹ have been paid much attention for this issue. Recently, reduced graphene oxide (rGO) has been proven as a good candidate for electrochemical sensing application among carbon-based materials, due to the fact that its honeycomb lattice molecular structure leads to remarkable physical and chemical properties, such as high surface area, high thermal and electrical conductivity, high chemical stability.³⁰⁻³³ Recent researches have shown that the electrochemical reduction of GO on working electrodes can be used to fabricate rGO-modified electrodes, which has been used for simultaneous electrochemical detection of AA, DA and UA.^{34,35} Additionally, the electrodeposition method for preparation of rGO-modified electrodes has an advantage of outstanding electronic conductivity between functional material and working electrode, compared to the method for drop coating of functional materials on working electrodes. However, the sensing performances of linear detection range and detection limit for simultaneous electrochemical detection of AA, DA and UA are relatively poor and need be further improved.

As we known, the improvement of sensing performances could be achieved by tuning the structure of the sensing materials. The introduction of carbon nanotube (CNT) into the matrix of rGO-based materials not only improves the electron transfer rate, but also produces additional porous structure, which is an effective method for enhancing the sensing performances. More recently, some results have been reported on addition of CNT in rGO-based materials for improvement the performances in various fields.³⁶⁻³⁸ However, the electrodeposition method for preparation of rGO-CNT hybrids modified ITO electrode for simultaneous electrochemical detection of AA, DA and UA has never been reported so far.

In this paper, rGO-CNT hybrids modified ITO (rGO-CNT/ITO) electrode has been successfully synthesized by

electrodeposition of GO stabilized CNT using ITO electrode as working electrode. Furthermore, the application of such rGO-CNT/ITO electrode has been examined for simultaneous electrochemical detection of AA, DA and UA, leading to a high-performance electrochemical sensor for simultaneous detection of AA, DA and UA.

Experimental

Materials and reagents

Graphite powder and DA were purchased from Aladin Ltd. (Shanghai, China). Multi-walled carbon nanotube (MWCNT) was purchased from Shenzhen Nanotech Port. NaNO₃ (99.0%), KMnO₄ (99%), K₃[Fe(CN)₆] (99%), NaH₂PO₄·2H₂O (99%), Na₂HPO₄·12H₂O (99%), AA and UA were purchased from Beijing Chemical Works (Beijing, China). KCl was purchased from Tianjin Kernel Chemical Reagents Development Centre (Tianjin, China). Silicone rubber was purchased from Zhonghao Chenguang Research Institute of Chemical Industry (Sichuan, China). The solvents including H₂SO₄ (98%) and H₂O₂ (30wt%) were supplied by Beijing Chemical Works (Beijing, China). All reagents were used directly without further purification. The deionized water used throughout all experiments was purified through a Millipore system. Potassium ferricyanide solution was prepared with 0.1 M KCl and 5 mM K₃[Fe(CN)₆]. Phosphate buffered saline (PBS) was prepared by mixing stock solutions of NaH₂PO₄ and Na₂HPO₄ and fresh solutions of AA, DA and UA were prepared daily.

Preparation of rGO-CNT/ITO electrode

An ITO conductive glass was cut to 6.0 cm x 0.6 cm and masked by silicone rubber, and used as the substrate for the electrochemical deposition of sensing materials. The GO-CNT aqueous dispersion was prepared by dispersing 11.0 mg of CNT and 5.0 mg of GO into 5.0 mL of 0.2 M PBS (pH 6.5) by sonication for 2 h. For the preparation of rGO-CNT/ITO electrode, 5.0 mL of GO-CNT dispersion was used as electrolyte. A conventional three-electrode cell was used, including an ITO (geometric area = 0.3 cm²) as the working electrode, a Ag/AgCl electrode as the reference electrode, and platinum foil as the counter electrode. Cyclic voltammetry (CV) was performed by scanning between 0 and -1.0 V at a rate of 50 mV s⁻¹. Then ITO modified by GO-CNT hybrids was taken off and rinsed with water three times lightly.

An additional reduction process had been performed to further reduce GO. In a typical run, 5.0 mL of 0.2 M PBS (pH 6.5) as electrolyte and same conventional three-electrode cell were used, including an ITO modified by GO-CNT hybrids as the working electrode, a Ag/AgCl electrode as the reference electrode, and platinum foil as the counter electrode. CV was performed by scanning between 0 and -1.0 V at a rate of 50 mV s⁻¹ with 10 potential cycles. Then ITO modified by rGO-CNT hybrids was taken off and rinsed with water three times lightly, and the resulting working electrode was rGO-CNT/ITO electrode for characterization and further use.

The rGO/ITO and CNT/ITO electrodes were also prepared by the similar method for preparation of rGO-CNT/ITO electrode in the absence of CNT and GO, respectively.

Characterizations

The morphology of rGO-CNT hybrids was observed by field emission scanning electron microscopy (FE-SEM) on a JSM-6700F electron microscope (JEOL, Japan). X-ray photoelectron spectroscopy (XPS) analysis was measured on an ESCALAB MK II X-ray photoelectron spectrometer using Mg as the exciting source. All the characterizations were performed by using GO-CNT/ITO and rGO-CNT/ITO as samples.

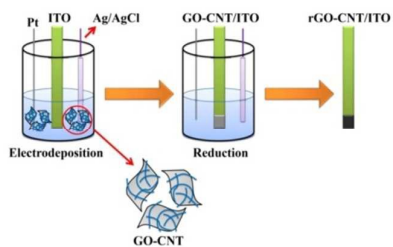
Electrochemical measurements were performed with a CHI 660D electrochemical analyzer (CH Instruments, Inc., Shanghai). A conventional three-electrode cell was used, including an ITO (geometric area = 0.3 cm²) as the working electrode, a Ag/AgCl electrode as the reference electrode, and platinum foil as the counter electrode. All the experiments were carried out at room temperature.

Results and discussion

Construction and characteristics of the rGO-CNT/ITO electrode

The synthetic route for rGO-CNT/ITO electrode is shown in Scheme 1. In the present work, GO-CNT dispersions were prepared as electrolyte and electrodeposition method was used to form GO-CNT layer on ITO surface. Subsequently, the additional reduction process had been performed to further reduce GO-CNT layer. Finally, rGO-CNT/ITO electrodes were constructed by assembly of rGO-CNT hybrids on ITO surface.

Fig. 1 shows the photographs of GO (5 mg), CNT (11 mg) and GO-CNT (5 mg and 11 mg, respectively) dispersions in 5 mL of 0.2 M PBS (pH 6.5), respectively. It is seen that GO is well-dispersed in PBS due to the abundant oxygen-containing groups. In contrast, aggregates are observed by addition of CNT into PBS due to the hydrophobicity of CNT. Interestingly, a stable dispersion is observed by addition of GO into the CNT dispersion, which could attributed to well dispersing ability of GO for CNT reported by the previous works.^{39,40}



Scheme 1 Schematic illustration of the fabrication and architecture of rGO-CNT/ITO.

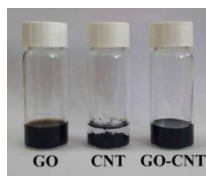


Fig. 1 The photographs of GO, CNT and GO-CNT dispersions.

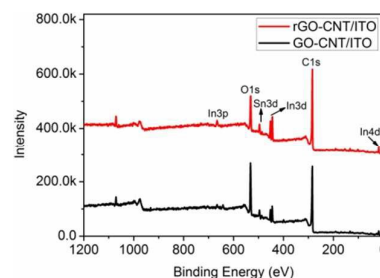


Fig. 2 XPS spectra of GO-CNT/ITO and rGO-CNT/ITO.

On the purpose of confirming the reduction of GO, XPS technique was used to characterize GO-CNT/ITO and rGO-CNT/ITO samples, which has been proven to be useful to analyze the chemical environment of carbon atoms in graphene-based materials. Fig. 2 shows XPS spectra of GO-CNT/ITO and rGO-CNT/ITO electrodes, respectively. It is seen that both samples exhibit two peaks at 284.6 and 531.9 eV, which are attributed to C1s and O1s bands, respectively. Additionally, the intensity of O1s band decreases for rGO-CNT/ITO sample compared with that of GO-CNT/ITO, indicating the removal of oxygen-containing groups in GO-CNT layer during the additional electrochemical reduction process. It is noted that GO-CNT/ITO and rGO-CNT/ITO samples also exhibit several bands associated with In3p, Sn3d, In3d and In4d bands, which are attributed to ITO substrate used. C1s spectra of GO-CNT/ITO and rGO-CNT/ITO samples are exhibited in Fig. 3a and b. It is seen that both samples exhibit three peaks at 284.6, 286.6 and 288.4 eV, which are associated with C-C, C-O and C=O, respectively. It is noted that the peak intensity of C-O and C=O in the C1s spectrum of rGO-CNT/ITO is lower than that of GO-CNT/ITO, indicating that oxygen-containing groups are successfully removed by electrochemical reduction. Furthermore, the ratios of carbon to oxygen of GO-CNT/ITO and rGO-CNT/ITO samples are 5.09 and 10.21, respectively. Notably, the ratio of carbon to oxygen of rGO-CNT/ITO sample is larger than that of GO-CNT/ITO sample, further indicating that the additional reduction process can remove oxygen-containing groups in GO-CNT/ITO sample.

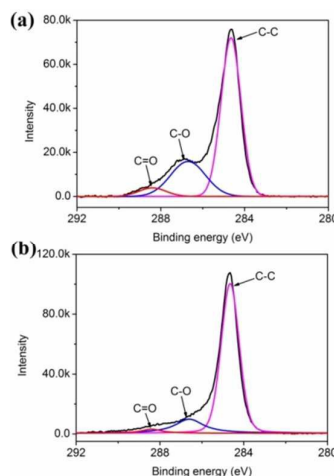


Fig. 3 C1s spectra of (a) GO-CNT/ITO and (b) rGO-CNT/ITO.

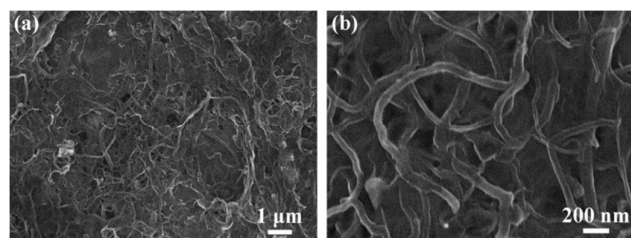


Fig. 4 (a) Low and (b) high magnification SEM images of the obtained rGO-CNT hybrids.

The morphology of the as-prepared rGO-CNT/ITO sample was characterized by SEM. Fig. 4a shows low magnification SEM image of rGO-CNT hybrids on ITO surface. It is seen that a uniform film is observed on rGO-CNT hybrids, which is attributed to the unique two-dimensional structure of rGO. Compared to the smooth surface of rGO film, rGO-CNT hybrids exhibit a relatively rough surface, where the smooth film is attributed to the rGO in the hybrids. Interestingly, a large amount of CNT with diameter of several tens of nanometers and length of a few micrometers are observed on rGO sheets, indicating the formation of rGO-CNT hybrids. The high magnification SEM image (Fig. 4b) further confirms the formation of rGO-CNT hybrids. This unique morphology is highly beneficial in maintaining large electroactive area on the electrode surface. All these results support the preparation of rGO-CNT hybrids by electrodeposition of GO-CNT dispersion on ITO, followed by additional electrochemical reduction process.

Electrochemical characterization of rGO-CNT/ITO electrode

Firstly, the electrodeposition process was investigated. Repetitive CVs in a potential range from 0 to -1.0 V for electrodeposition process of GO-CNT on ITO are shown in Fig. S1. The considerably large cathodic current starting at a potential of about -0.8 V are observed. Furthermore, the intensities of current increase with the progression of cycling, suggesting the electrodeposition of GO-CNT in progress. Fig. S2 shows CVs of GO-CNT/ITO electrode with 10 potential cycles in 0.2 M PBS (pH 6.5). As similar to the electrochemical reduction behaviors of GO,^{34,41} the reduction peak at -0.95 V is observed in the first cycle. From the second cycle, the intensities of reduction current decrease with the progression of cycling and reach a plateau in last cycles, indicating the electrochemical reduction of GO-CNT.

Subsequently, the electrochemical activity of as-prepared rGO-CNT/ITO electrodes is examined by the electrochemical catalytic reactions between $\text{Fe}(\text{CN})_6^{4-}$ and $\text{Fe}(\text{CN})_6^{3-}$. Fig. 5a shows CVs of bare ITO electrode and rGO-CNT/ITO electrode with various contents of GO-CNT hybrids in potassium ferricyanide solution (scan rate: 0.1 V s^{-1}). The contents of GO-CNT hybrids on ITO were controlled by tuning potential cycles. It is seen that the oxidation peaks attributed to oxidation of $\text{Fe}(\text{CN})_6^{4-}$ and the reduction peaks attributed to reduction of $\text{Fe}(\text{CN})_6^{3-}$ are observed on bare ITO electrode at 0.33 V and 0.11 V, respectively. The peak currents increase after deposition of GO-CNT dispersion on ITO, indicating the improvement of electron transferring due to the presence of

rGO-CNT hybrids. Furthermore, such peak currents increase with increasing potential cycle from 0 to 10 and reach a maximum at potential cycle of 10. The further increasing potential cycle results in decreasing the peak currents for the redox. This result indicates that the electrochemical activity of ITO electrode is improved by electrodeposition of rGO-CNT hybrids and the fasted electronic transmission is obtained at the loading amount of deposits by 10 potential cycles.

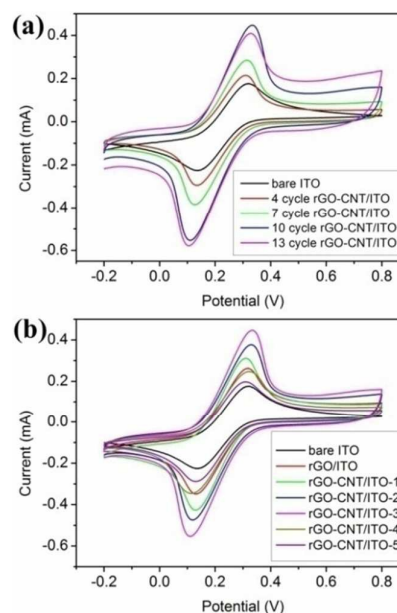


Fig. 5 (a) CVs of bare ITO electrode and rGO-CNT/ITO electrode with various contents of GO-CNT hybrids in potassium ferricyanide solution; (b) CVs of bare ITO electrode, rGO/ITO electrode and rGO-CNT/ITO electrode with various ratios of CNT to GO in potassium ferricyanide solution. (scan rate: 0.1 V s^{-1})

Table 1 Comparison of the proportion of CNT to affect the electrochemical activity of hybrids.

Sample	CNT:GO ^a	Oxidation peak current (mA)
rGO/ITO	0:1	0.26
rGO-CNT/ITO-1	0.6:1	0.31
rGO-CNT/ITO-2	1.4:1	0.37
rGO-CNT/ITO-3	2.2:1	0.44
rGO-CNT/ITO-4	3.0:1	0.24
rGO-CNT/ITO-5	3.8:1	0.19

^a CNT:GO-mass ratio of CNT to GO.

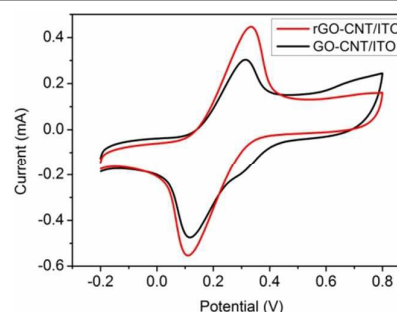


Fig. 6 CVs of GO-CNT/ITO electrode and rGO-CNT/ITO electrode in potassium ferricyanide solution. (scan rate: 0.1 V s^{-1})

The proportion of CNT in rGO-CNT hybrids to affect the electrochemical activity of hybrids is focus of discussion. Fig. 5b shows CVs of bare ITO electrode, rGO/ITO electrode and rGO-CNT/ITO electrode with various ratios of CNT to GO in potassium ferricyanide solution. The different proportions of CNT in rGO-CNT have been controlled by the synthesis of GO-CNT dispersions with various ratios of CNT to GO, as shown in Table 1. It is seen that the oxidation peak currents increase with increasing ratio of CNT to GO from 0 to 2.2 and reach a maximum at mass ratio of CNT to GO about 2.2. Then, the oxidation peak currents decrease by further increasing the ratio of CNT to GO from 2.2 to 3.8. This result indicates that addition of CNT can effectively improve the electrochemical activity of rGO. However, relatively high contents of CNT could hinder the electrodeposition of rGO-CNT hybrids on ITO surface, which leading to decreasing electrochemical activity of modified electrodes. The CV of CNT/ITO electrode was also investigated in the same conditions, as shown in Fig. S3. The oxidation peak current of CNT/ITO electrode is lower than that of rGO-CNT/ITO. The result further reveals the enhanced electrochemical performance of the combined rGO with CNT. The rGO-CNT hybrids take dual advantages of CNT and rGO. According to the previous reports,^{40,42} the assembly with CNT can hinder restacking of rGO and the introduction of CNT is thought to effectively improve the electron transport of rGO-CNT hybrids owing to their good conductivity. At the same time, the microstructure of the rGO-CNT architecture provides sufficient space and sites for the redox reaction between $\text{Fe}(\text{CN})_6^{4-}$ and $\text{Fe}(\text{CN})_6^{3-}$, and to accelerate the reduction rate. Attributed to the uniform structure and improved electrical conductivity, rGO-CNT hybrids exhibit highly enhanced electrochemical performance compared with that of rGO and CNT.

In addition, the effect of additional reduction process on the electrochemical sensing of rGO-CNT/ITO electrode is also examined. Fig. 6 shows CVs of GO-CNT/ITO electrode and rGO-CNT/ITO electrode in potassium ferricyanide solution. It is seen that the peak currents of rGO-CNT/ITO are higher than that of GO-CNT/ITO. This result indicates that the reduction process can further improve the electrochemical activity, where GO in the GO-CNT was reduced to construct rGO-CNT hybrids. All results exhibit that the addition of CNT can improve the electrochemical activity of rGO and the electrochemical activity of rGO-CNT/ITO electrode can be adjusted by controlling the loading amount of deposits and the proportion of CNT in rGO-CNT hybrids.

The electrochemical sensor based on rGO-CNT hybrids was constructed for simultaneous electrochemical detection of AA, DA and UA. Firstly, the individual electrochemical behaviors of AA, DA and UA are examined. Fig. 7a shows CVs of bare ITO electrode, rGO/ITO electrode and rGO-CNT/ITO electrode in 0.1 M PBS (pH 7.0) containing 1 mM AA (scan rate: 50 mV s⁻¹). It is seen that the response of bare ITO electrode to AA is pretty weak. In contrast, the rGO-CNT/ITO exhibits remarkable oxidation current peak about 234 μA at 0.04 V, indicating that rGO-CNT hybrids could detect electrochemical oxidation of AA. Furthermore, the oxidation current peak of rGO/ITO about

106 μA at 0.07 V is lower than that of rGO-CNT/ITO, indicating the enhancing the sensing performances of rGO-CNT hybrids by introduction of CNT for electrochemical detection of AA. The redox behavior of DA on various electrodes is shown in Fig. 7b. The oxidation peak current of bare ITO electrode to 0.1 mM DA is 15 μA at 0.56 V. Notably, the oxidation peak current of rGO-CNT/ITO is 190 μA at 0.24 V, which is much higher than that of bare ITO electrode, as well as rGO/ITO electrode (101 μA at 0.23 V). This result indicates that electrochemical redox of DA has been strongly improved by rGO-CNT/ITO electrode, which is attributed to the introduction of CNT into the matrix of rGO, especially, compared to rGO/ITO electrode. Fig. 7c shows the response of 0.1 mM UA at different electrodes. The response of bare ITO electrode to UA can be observed hardly. In contrast, the remarkable oxidation current peak of rGO-CNT/ITO locates at 0.37 V about 155 μA , indicating that rGO-CNT/ITO electrode exhibits good catalytic activity for electrochemical oxidation of UA. The oxidation peak current of rGO/ITO is 83 μA at 0.37 V, which is lower than that of rGO-CNT/ITO, indicating that the addition of CNT can improve the sensing performances of rGO for electrochemical detection of UA.

Subsequently, simultaneous electrochemical detection of AA, DA and UA is examined by CV technique. Fig. 7d shows CVs of different electrodes in PBS containing 1 mM AA, 0.1 mM DA and 0.1 mM UA. Only one oxidation peak is observed on CVs of bare ITO and CNT/ITO (as shown in Fig. S4), indicating that bare ITO and CNT/ITO could not identify AA, DA and UA in detail. In contrast, three oxidation current peaks of rGO-CNT/ITO can be distinguished easily, which are attributed to oxidation of AA located at 0.04 V about 168 μA , oxidation of DA located at 0.28 V about 303 μA and oxidation of UA located at 0.38 V about 230 μA , respectively. This result indicates that the simultaneous electrochemical detection of AA, DA and UA can be performed by using rGO-CNT/ITO electrode. Furthermore, the three oxidation current peaks of rGO/ITO attributed to oxidation of AA, DA and UA are about 100, 147 and 103 μA at 0.07, 0.25 and 0.35 V, respectively. Such oxidation current peaks are lower than that of rGO-CNT/ITO, respectively, and the oxidation current peak of UA at rGO/ITO electrode is relatively difficult to distinguish. This result indicates the enhancing the sensing performances of rGO-CNT hybrids by introduction of CNT for simultaneous electrochemical detection of AA, DA and UA.

In order to evaluate the kinetics of electrode reaction, the scan rates have been investigated. Fig. S5a shows the CVs of rGO-CNT/ITO electrode in 0.1 M PBS (pH 7.0) with 1 mM AA at scan rates from 10 to 100 mV s⁻¹. It is seen that the oxidation peak current gradually increases with the increase of scan rates. The linear relation has been established between the oxidation peak current and the square root of scan rate, as shown in Fig. S5b, indicating the diffusion-controlled processes for detection of AA. Furthermore, the effect of scan rate on sensing performances of rGO-CNT/ITO for detection of DA and UA was also examined, as shown in Fig. S5c-f, indicating the diffusion-controlled processes for detection of DA and UA, respectively.⁴³⁻⁴⁵

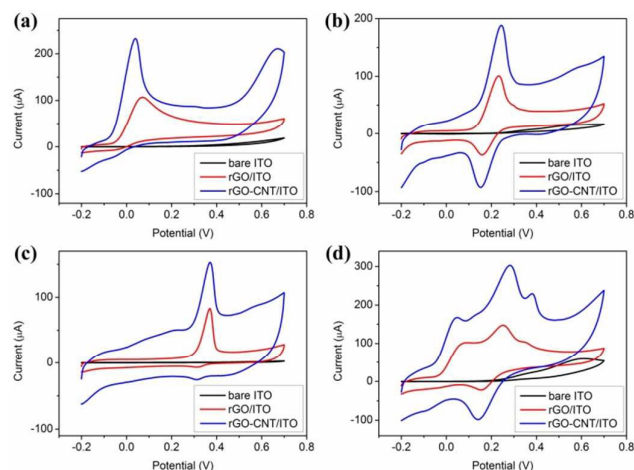


Fig. 7 CVs of bare ITO electrode, rGO/ITO electrode and rGO-CNT/ITO electrode in 0.1 M PBS (pH 7.0) (a) containing 1 mM AA; (b) containing 0.1 mM DA; (c) containing 0.1 mM UA; (d) containing 1 mM AA, 0.1 mM DA and 0.1 mM UA. (scan rate: 50 mV s^{-1})

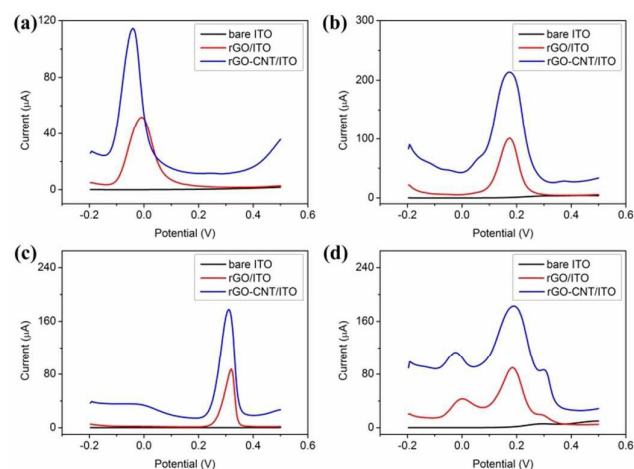


Fig. 8 DPVs of bare ITO electrode, rGO/ITO electrode and rGO-CNT/ITO electrode in 0.1 M PBS (pH 7.0) (a) containing 1 mM AA; (b) containing 0.1 mM DA; (c) containing 0.1 mM UA; (d) containing 1 mM AA, 0.1 mM DA and 0.1 mM UA.

The individual electrochemical behaviors of AA, DA and UA are further studied by using differential pulse voltammetry (DPV). The DPVs of bare ITO electrode, rGO/ITO electrode and rGO-CNT/ITO electrode for detection of AA are displayed, as shown in Fig. 8a. The response of rGO-CNT/ITO to 1 mM AA is $115 \mu\text{A}$ at -0.04 V , which is more remarkable than that of bare ITO and rGO/ITO ($51 \mu\text{A}$ located at -0.01 V). Fig. 8b shows DPVs of different electrodes in PBS containing 0.1 mM DA. It is seen that the response of rGO/ITO and rGO-CNT/ITO to DA are $101 \mu\text{A}$ and $214 \mu\text{A}$, respectively, and both of them locate at 0.17 V . Compared with the oxidation current peaks of bare ITO electrode and rGO/ITO electrode, the oxidation current peak of rGO-CNT/ITO electrode shows higher intensity than the other ones, indicating that rGO-CNT/ITO electrode can more effectively detect DA. The oxidation behavior of UA is examined by DPV, as shown in Fig. 8c. It can be seen that the DPV of bare ITO for detection of 0.1 mM UA is a straight

line, and the oxidation current peak of rGO/ITO is $88 \mu\text{A}$ located at 0.32 V . In contrast, the rGO-CNT/ITO exhibits remarkable oxidation current peak about $178 \mu\text{A}$ at 0.31 V , further indicating the enhancing the sensing performances of rGO-CNT hybrids for electrochemical detection of UA.

Subsequently, simultaneous electrochemical detection of AA, DA and UA is examined by using DPV. Fig. 8d shows DPVs of bare ITO electrode, rGO/ITO electrode and rGO-CNT/ITO electrode in PBS containing 1 mM AA, 0.1 mM DA and 0.1 mM UA. It is seen that the oxidation of AA, DA and UA at ITO electrode exhibit similar oxidation potentials, revealing only one weak oxidation peak. In contrast, the oxidation of AA, DA and UA at rGO-CNT/ITO electrode can be identified, and three oxidation current peaks of DPV are attributed to oxidation of AA ($114 \mu\text{A}$ located at -0.03 V), DA ($184 \mu\text{A}$ located at 0.19 V) and UA ($88 \mu\text{A}$ located at 0.31 V). This result indicates that rGO-CNT/ITO electrode can simultaneously detect AA, DA and UA by using DPV. The oxidation of AA, DA and UA at CNT/ITO electrode can be distinguish hardly, as shown in Fig. S6, revealing that the CNT/ITO electrode is not suitable for simultaneous electrochemical detection of AA, DA and UA. Furthermore, the oxidation current peaks of AA, DA and UA at rGO/ITO electrode are 43 , 89 and $19 \mu\text{A}$ located at -0.01 , 0.19 and 0.29 V , and the peak potential separations for AA-DA and DA-UA in DPV at rGO/ITO electrode are 183 and 106 mV , respectively. The oxidation current peaks of rGO-CNT/ITO are higher than that of rGO/ITO, and the peak potential separations for AA-DA (215 mV) and DA-UA (114 mV) at rGO-CNT/ITO electrode are wider than that at rGO/ITO electrode, further indicating the enhancing the sensing performances of rGO-CNT hybrids by introduction of CNT. All results exhibit that the addition of CNT can improve the sensing performances of rGO. Hence, the rGO-CNT hybrids could be used as a promising material for fabrication of AA, DA and UA sensor.

The linear detection ranges and detection limits of AA, DA and UA sensor based on rGO-CNT hybrids are examined by DPVs. Fig. 9a shows DPVs at rGO-CNT/ITO in 0.1 M PBS (pH 7.0) containing $5 \mu\text{M}$ DA, $10 \mu\text{M}$ UA, and different concentrations of AA. It is seen that the peak currents attributed to oxidation of AA enhance gradually with adding AA from $10 \mu\text{M}$ to $200 \mu\text{M}$. As shown in Fig. 9b, the oxidation peak currents of AA increase linearly with the increase of AA concentration from $10 \mu\text{M}$ to $200 \mu\text{M}$ ($R = 0.997$). The detection limit for AA was estimated to be $5.31 \mu\text{M}$ at a signal-to-noise ratio of 3. Fig. 9c shows DPVs at rGO-CNT/ITO in PBS containing $500 \mu\text{M}$ AA, $10 \mu\text{M}$ UA, and different concentrations of DA. The linear relationship between the peak currents and DA concentrations is obtained in the range of 0.2 – $8.0 \mu\text{M}$ ($R = 0.996$), as shown in Fig. 9d. The detection limit ($S/N = 3$) for DA is $0.04 \mu\text{M}$. Similarly, the oxidation current peaks of UA enhance gradually by increasing the concentrations of UA, as shown in Fig. 9e. The peak currents of UA increase linearly with the increase of UA concentration from $0.2 \mu\text{M}$ to $16.0 \mu\text{M}$ ($R = 0.999$), as shown in Fig. 9f. The detection limit ($S/N = 3$) for UA is $0.17 \mu\text{M}$.

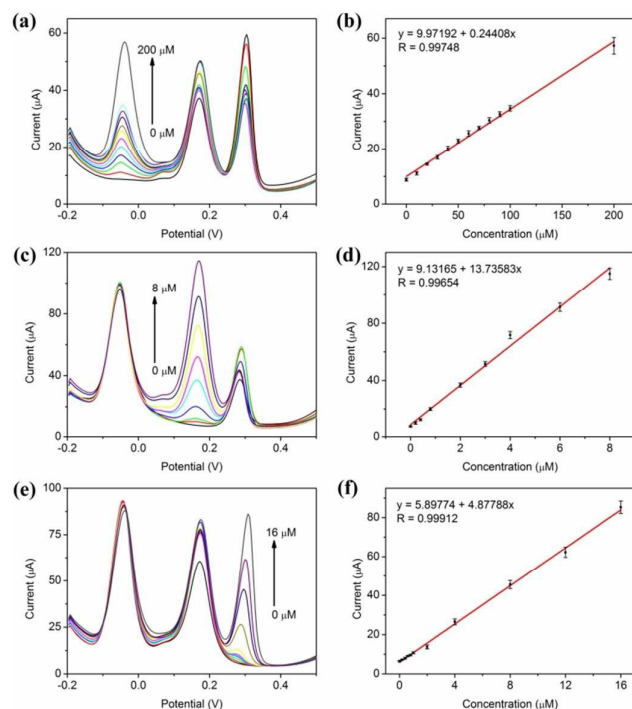


Fig. 9 DPVs at rGO-CNT/ITO electrode in 0.1 M PBS (pH 7.0) (a) containing 5 μM DA, 10 μM UA, and different concentrations of AA: 0, 10, 20, 30, 40, 50, 60, 70, 80, 90, 100, 200 μM ; (b) calibration plot of the concentration of AA versus peak current; (c) containing 500 μM AA, 10 μM UA, and different concentrations of DA: 0, 0.2, 0.4, 0.8, 2, 3, 4, 6, 8 μM ; (d) calibration plot of the concentration of DA versus peak current; (e) containing 500 μM AA, 5 μM DA, and different concentrations of UA: 0, 0.2, 0.4, 0.6, 0.8, 1, 2, 4, 8, 12, 16 μM ; (f) calibration plot of the concentration of UA versus peak current.

To investigate the anti-interference of rGO-CNT/ITO, several co-existing substances were added for detection of AA, DA and UA, including NaCl (50 mM), KCl (50 mM), NaNO₃ (50 mM), NaNO₂ (50 mM) and glucose (20 mM), as shown in Fig. S7. It can be found that no significant interference for the detection of AA (100 μM), DA (3 μM) and UA (5 μM) was observed from those compounds. In addition, the sensing performances based on rGO-CNT hybrids were compared with the previously reported based on rGO-based or CNT-based materials for simultaneous electrochemical detection of AA, DA and UA, as shown in Table S1. It is seen that the linear range for DA at rGO-CNT/ITO (0.2–8 μM) is wider than that at SWCNH/GCE³ (0.2–3.8 μM). The detection limit for AA at rGO-CNT/ITO (5.31 μM) is lower than that at MWCNT/CCE²⁹ (7.71 μM) and ERGO/GCE³⁴ (250 μM). The detection limit for UA at rGO-CNT/ITO (0.17 μM) is lower than that at HCNTs/GCE¹¹ (1.5 μM), MWCNT/CCE (0.42 μM), ERGO/GCE (0.5 μM) and rGO/GCE³⁵ (1 μM). Especially for DA, the detection limit at rGO-CNT/ITO (0.04 μM) is lower than that at those based on rGO-based or CNT-based materials. The mixing of rGO and CNT material exhibits excellent performances for simultaneous electrochemical detection of AA, DA and UA in our work.

The stability, reproducibility and repeatability of rGO-CNT/ITO are also examined. The rGO-CNT/ITO remained 92%, 93% and 90% of its initial DPVs to 1 mM AA, 0.1 mM

DA and 0.1 mM UA after 10 days' storage, respectively, indicating the good stability of rGO-CNT/ITO electrode. The reproducibility was estimated from DPVs to detect 1 mM AA, 0.1 mM DA and 0.1 mM UA at five electrodes prepared in the same conditions and relative standard deviation (RSD) of 4.8%, 3.5% and 4.1% were obtained, respectively. The peak currents of DPVs at rGO-CNT/ITO were recorded for 5 successive measurements, RSD of 1 mM AA, 0.1 mM DA and 0.1 mM UA are 2.9%, 2.7% and 3.1%, respectively, indicating the good repeatability of rGO-CNT/ITO.

To examine the accuracy and applicability of rGO-CNT/ITO, the application of rGO-CNT/ITO electrode for simultaneous detection of AA, DA and UA in human urine was investigated. The urine sample was diluted 40 times with 0.1 M PBS (pH 7.0), and no other pretreatment process was performed. (results as shown in Table S2) It is seen that the recoveries are 95.7%, 102.4% and 96.4% for 100 μM AA, 5 μM DA and 5 μM UA, respectively, suggesting the potential application for simultaneous detection of AA, DA and UA in real samples.

Conclusions

In summary, rGO-CNT hybrids have been successfully prepared by electrodeposition of GO stabilizing CNT and electrochemical reduction of GO-CNT hybrids on ITO surface, and such hybrids are first used for simultaneous electrochemical detection of AA, DA and UA. As-prepared rGO-CNT/ITO electrodes exhibit excellent electrochemical activity and sensing performances. Our present work provides a simple, novel, low-cost and environmental friendly method for development of high performance electrochemical sensors using carbon-based materials.

Acknowledgements

This research work was financially supported by the National Natural Science Foundation of China (Grant No. 51202085) and the Open Project from State Key Laboratory of Transducer Technology (Grant No. SKT1402).

References

- 1 C.-L. Sun, C.-T. Chang, H.-H. Lee, J. Zhou, J. Wang, T.-K. Sham and W.-F. Pong, *ACS Nano*, 2011, **5**, 7788–7795.
- 2 P. Gai, H. Zhang, Y. Zhang, W. Liu, G. Zhu, X. Zhang and J. Chen, *J. Mater. Chem. B*, 2013, **1**, 2742–2749.
- 3 S. Zhu, H. Li, W. Niu and G. Xu, *Biosens. Bioelectron.*, 2009, **25**, 940–943.
- 4 C. Xiao, X. Chu, Y. Yang, X. Li, X. Zhang and J. Chen, *Biosens. Bioelectron.*, 2011, **26**, 2934–2939.
- 5 D. Zhang, R. Zhang, C. Xu, Y. Fan and B. Yuan, *Sens. Actuators B*, 2015, **206**, 1–7.
- 6 L. Wang, X. Lu, C. When, Y. Xie, L. Miao, S. Chen, H. Li, P. Li and Y. Song, *J. Mater. Chem. A*, 2015, **3**, 608–616.
- 7 J. Song, L. Xu, R. Xing, Q. Li, C. Zhou, D. Liu and H. Song, *Sci. Rep.*, 2014, **4**, 7515.
- 8 S. Liu, B. Yu and T. Zhang, *J. Mater. Chem. A*, 2013, **1**, 13314–13320.

- 9 M. Noroozifar, M. Khorasani-Motlagh and A. Taheri, *Talanta*, 2010, **80**, 1657-1664.
- 10 C.-L. Sun, H.-H. Lee, J.-M. Yang and C.-C. Wu, *Biosens. Bioelectron.*, 2011, **26**, 3450-3455.
- 11 R. Cui, X. Wang, G. Zhang and C. Wang, *Sens. Actuators B*, 2012, **161**, 1139-1143.
- 12 Z.-H. Sheng, X.-Q. Zheng, J.-Y. Xu, W.-J. Bao, F.-B. Wang and X.-H. Xia, *Biosens. Bioelectron.*, 2012, **34**, 125-131.
- 13 Y. Liu, J. Huang, H. Hou and T. You, *Electrochem. Commun.*, 2008, **10**, 1431-1434.
- 14 A. A. Rafati, A. Afraz, A. Hajian and P. Assari, *Microchim. Acta*, 2014, **181**, 1999-2008.
- 15 Y. Yue, G. Hu, M. Zheng, Y. Guo, J. Cao and S. Shao, *Carbon*, 2012, **50**, 107-114.
- 16 R. P. Silva, A. W.O. Lima and S. H.P. Serrano, *Anal. Chim. Acta*, 2008, **612**, 89-98.
- 17 Z. Wang, M. Shoji and H. Ogata, *Analyst*, 2011, **136**, 4903-4905.
- 18 A. Walcarius, S. D. Minter, J. Wang, Y. Lin and A. Merkoci, *J. Mater. Chem. B*, 2013, **1**, 4878-4908.
- 19 B. Yuan, C. Xu, L. Liu, Y. Shi, S. Li, R. Zhang and D. Zhang, *Sens. Actuators B*, 2014, **198**, 55-61.
- 20 M. K. Kundu, M. Sadhukhan and S. Barman, *J. Mater. Chem. B*, 2015, **3**, 1289-1300.
- 21 L. Wang, Y. Zheng, X. Lu, Z. Li, L. Sun and Y. Song, *Sens. Actuators B*, 2014, **195**, 1-7.
- 22 B. Zhuo, Y. Li, A. Zhang, F. Lu, Y. Chen and W. Gao, *J. Mater. Chem. B*, 2014, **2**, 3263-3270.
- 23 S. Thiagarajan and S.-M. Chen, *Talanta*, 2007, **74**, 212-222.
- 24 Y. Li and X. Lin, *Sens. Actuators B*, 2006, **115**, 134-139.
- 25 A. A. Ensafi, M. Taei, T. Khayamian and A. Arabzadeh, *Sens. Actuators B*, 2010, **147**, 213-221.
- 26 J. Yan, S. Liu, Z. Zhang, G. He, P. Zhou, H. Liang, L. Tian, X. Zhou and H. Jiang, *Colloids Surf. B*, 2013, **111**, 392-397.
- 27 G. Wang, J. Sun, W. Zhang, S. Jiao and B. Fang, *Microchim. Acta*, 2009, **164**, 357-362.
- 28 M. Li, W. Guo, H. Li, W. Dai and B. Yang, *Sens. Actuators B*, 2014, **204**, 629-636.
- 29 B. Habibi and M. H. Pournaghi-Azar, *Electrochim. Acta*, 2010, **55**, 5492-5498.
- 30 H.-J. Lee, E. Kim, J. Park, W. Song, K.-S. An, Y. S. Kim, J.-G. Yook and J. Jung, *Carbon*, 2014, **78**, 532-539.
- 31 R. Devasenathipathy, V. Mani and S.-M. Chen, *Talanta*, 2014, **124**, 43-51.
- 32 M. Sadhukhan, T. Bhowmik, M. K. Kundu and S. Barman, *RSC Adv.*, 2014, **4**, 4998-5005.
- 33 E. Kim, Y. S. Kim, J. Park, S. Hussain, S.-H. Chun, S. J. Kim, K.-S. An, W.-J. Lee, W.-G. Lee and J. Jung, *RSC Adv.*, 2014, **4**, 63349-63353.
- 34 L. Yang, D. Liu, J. Huang and T. You, *Sens. Actuators B*, 2014, **193**, 166-172.
- 35 H. Wang, F. Ren, C. Wang, B. Yang, D. Bin, K. Zhang and Y. Du, *RSC Adv.*, 2014, **4**, 26895-26901.
- 36 X. Fan, G. Jiao, L. Gao, P. Jin and X. Li, *J. Mater. Chem. B*, 2013, **1**, 2658-2664.
- 37 J. Qian, X. Yang, Z. Yang, G. Zhu, H. Mao and K. Wang, *J. Mater. Chem. B*, 2015, **3**, 1624-1632.
- 38 K.-Y. Hwa and B. Subramani, *Biosens. Bioelectron.*, 2014, **62**, 127-133.
- 39 C. Zhang, L. Ren, X. Wang and T. Liu, *J. Phys. Chem. C*, 2010, **114**, 11435-11440.
- 40 T. Sun, Z. Zhang, J. Xiao, C. Chen, F. Xiao, S. Wang and Y. Liu, *Sci. Rep.*, 2013, **3**, 2527.
- 41 J. Yang, J. R. Strickler and S. Gunasekaran, *Nanoscale*, 2012, **4**, 4594-4602.
- 42 C. H. Choi, M. W. Chung, H. C. Kwon, J. H. Chung and S. I. Woo, *Appl. Catal. B Environ.*, 2014, **144**, 760-766.
- 43 H. Wang, C. Wang, B. Yang, C. Zhai, D. Bin, K. Zhang, P. Yang and Y. Du, *Analyst*, 2015, **140**, 1291-1297.
- 44 C. Wang, J. Du, H. Wang, C. Zou, F. Jiang, P. Yang and Y. Du, *Sens. Actuators B*, 2014, **204**, 302-309.
- 45 B. Yang, H. Wang, J. Du, Y. Fu, P. Yang and Y. Du, *Colloids Surf., A: Physicochem. Eng. Aspects*, 2014, **456**, 146-152.